Molecular Systems Design & Engineering

COMMUNICATION

View Article Online
View Journal | View Issue

Cite this: *Mol. Syst. Des. Eng.*, 2016, **1**, 169

Received 17th November 2015,
Accepted 4th January 2016

DOI: 10.1039/c5me00006h

rsc.li/molecular-engineering

Robust control over morphologies and grain interfaces of three-dimensional well-ordered superstructures programmed by hybrid topographical-chemical templates†

Zhinan Cong, Liangshun Zhang,* Liquan Wang and Jiaping Lin*

It is an extremely challenging task to construct three-dimensional (3D) well-ordered superstructures with controllable morphologies and predictable internal components. Using computational modeling, we conceive and demonstrate a novel class of templates with topographically and chemically patterned surfaces for directing the self-assembly of symmetric block copolymers. Large-cell simulations of self-consistent field theory corroborate that 3D sophisticated structures of vertical lamellae with different in-plane orientations are achieved and the placements of grain interfaces are regulated by post height and commensurability conditions. Notably, non-orthogonally crossed structures are created by simply modulating the periodicities of post arrays. This work may provide a novel route for experimentalists to fabricate 3D long-range ordered structures with tunable local characteristics.

Introduction

The true potential of block copolymers in the semiconductor industry is likely to come from the inherently three-dimensional (3D) characteristics of microphase-separated nanostructures,[1,2] which allow researchers to construct 3D ordered superstructures in a single self-assembly step. Directed self-assembly structures with 3D sophisticated features provide an enabling platform for nanofabrication of electronic, magnetic or photonic devices.[3,4] However, creating 3D ordered nanostructures that simultaneously possess controllable morphologies as well as precisely arranged internal components (such as interconnections and grain interfaces) still remains challenging.[5,6]

Recent efforts of experiments and simulations have shown that the guiding templates for directed self-assembly play a critical role in building up 3D well-ordered structures of block copolymers.[7–10] For example, Ross and co-workers designed a rectangular array of topographical posts to program the 3D superstructures of cylinder-forming block copolymer bilayer films.[11–14] Unlike the case of the bulk structure, the orientations of cylinders in the top and bottom layers are regulated simultaneously and independently. Nevertheless, the vertical interconnections between the crossing cylinders, which play an important role in improving the performance and power of 3D integrated-circuit systems,[15] are formed in a limited range of design elements of guiding templates, such as film thickness, post height and wetting properties of surfaces.[14,16]

Another approach to achieve 3D highly ordered architectures is based on the utilization of chemical stripes.[17,18] Since their top surfaces cannot eliminate possible orientations, block copolymers guided by mismatched chemical stripes self-assemble into non-bulk structures containing many degenerate states.[8,19–21] In the group of de Pablo, 3D twisted structures with continuity of lamellae and interconnections are elaborately realized through the self-assembly of symmetric block copolymers directed by templates with two orthogonally oriented chemically patterned surfaces.[22,23] Unfortunately, as the films become thick, the interfaces separating the grains of the lamellae are randomly distributed inside the 3D structures due to the short-range guiding characteristics of chemical stripes. This poses a significant stumbling block to achieve controllable morphologies of 3D structures with precise placements of grain interface, which foreshadow the potential to fabricate 3D integrated-circuit elements, photovoltaic devices and energy storage devices.[23]

In this contribution, we theoretically engineer novel templates, which combine top chemically and bottom topographically patterned surfaces, to direct the self-assembly of lamella-forming block copolymers. In comparison with the templates mentioned above, the key advantage of the hybrid templates is that the morphologies of complex 3D structures could be robustly and flexibly controlled by post height and

Shanghai Key Laboratory of Advanced Polymeric Materials, State Key Laboratory of Bioreactor Engineering, Key Laboratory for Ultrafine Materials of Ministry of Education, School of Materials Science and Engineering, East China University of Science and Technology, Shanghai 200237, China. E-mail: zhangls@ecust.edu.cn, jlin@ecust.edu.cn

† Electronic supplementary information (ESI) available. See DOI: 10.1039/c5me00006h

commensurability conditions, and the grain interfaces in the 3D long-range ordered nanostructures could be restricted to the narrow zones of films. In addition, the hybrid templates facilitate the formation of non-orthogonally crossed architectures by simply tuning the periodicities of topographical posts.

Computational modeling

Full technical details of the model can be found in Part A and Fig. S1 of ESI.† In brief, AB block copolymers are confined between the top and bottom surfaces as schematically illustrated in Fig. 1. Two types of templates are explored in the simulations. Fig. 1a displays the templates consisting of two chemically patterned surfaces with orthogonal orientations. In the hybrid templates, the bottom chemical stripes are replaced with topographical posts (Fig. 1b). We utilize the self-consistent field theory (SCFT) of polymers to probe into the directed self-assembly behaviors of the block copolymers.[24,25] The Flory–Huggins interaction parameter between the A and B blocks is set as χN = 14.0. In the bulk structure, the symmetric block copolymers self-assemble into the lamellae with a natural periodicity $L_0 \sim 3.6R_g$, where R_g is the ideal gyration radius. The interaction parameters between the blocks and the surfaces are fixed at λN = 10.0. For the posts modeled by external fields, the changes at the well edge for the A and B blocks are respectively set as $0.10R_g$ and $0.20R_g$, implying that the posts are weakly attractive to the A blocks.

Results and discussion

We first observe the ordered superstructures of block copolymer films in the chemical templates. Fig. 2a and b show the morphologies of the 3D structures of the block copolymer films with thicknesses of $H = 4.0R_g$ and $H = 6.5R_g$, respectively. The two chemical stripes on the top and bottom surfaces direct the block copolymers to self-assemble into grains of lamellae perpendicular to the surfaces. Due to the orthogonally oriented stripes, the two lamellar grains are twisted inside the films (inset of Fig. 2a), producing 3D structures with continuity of nanodomains. The grains of lamellae with different in-plane orientations are separated by interfaces (the positions are marked by the planes enclosed in the white boxes, as shown in Fig. 2b). From the 3D views of superstructures, one can identify that the film thickness has a significant effect on the positions of the grain interfaces. In the cases of thin films, the locations of the interfaces are restricted to the center of the films (Fig. 2a). However, the interfaces are delocalized away from the middle of the thick films (Fig. 2b).

To quantitatively measure the localizations of the interfaces in the 3D structures, we introduce position parameters (m) to characterize the positions of the interfaces separating the lamellar grains in the unit cells (V_0),[26] which have different domains on the top and bottom surfaces, as shown in Fig. 2b. The grain interfaces located at the center of the cells (V_0) will result in m = 0. When the position parameters (m)

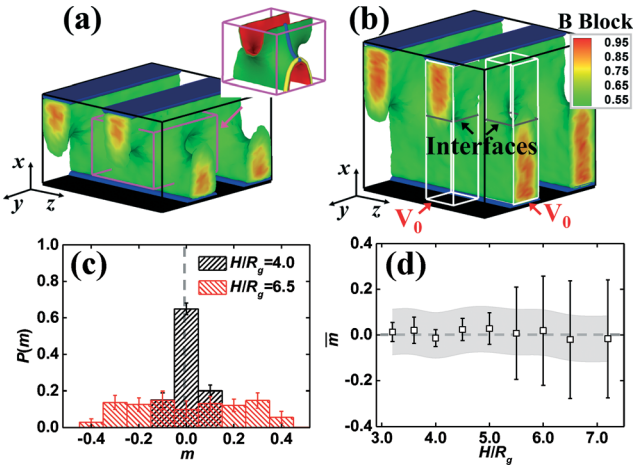

Fig. 2 (a and b) Three-dimensional ordered structures of block copolymers guided by chemical templates with a stripe width of $W_s = 1.8R_g$ and periodicity of $L_s = 3.6R_g$ at various film thicknesses ((a) $H = 4.0R_g$ and (b) $H = 6.5R_g$). The A-rich domains and top surfaces are removed for visualization purposes. In the color bar, the red and green colors indicate the B-rich domains and internal interfaces between the A-rich and B-rich domains, respectively. The inset of panel (a) displays the zoomed-in image of the internal surface at the orientation transition of lamellae, and the blue and yellow curves show the two representative curves across the saddle points of Scherk's surfaces. In image (b), the planes enclosed in the unit cells (V_0) represent the positions of the grain interfaces. (c) Probability distributions ($P(m)$) of the position parameter (m) at different film thicknesses ($H = 4.0R_g$ and $H = 6.5R_g$). (d) Averaged position parameters ($\bar{m}$) of the three-dimensional structures as a function of film thickness. The error bars represent the standard deviations. The dashed lines at m = 0.0 indicate the grain interfaces located at the center of films. The filled area in image (d) indicates that the standard deviations from the averaged position parameters are less than 0.1.

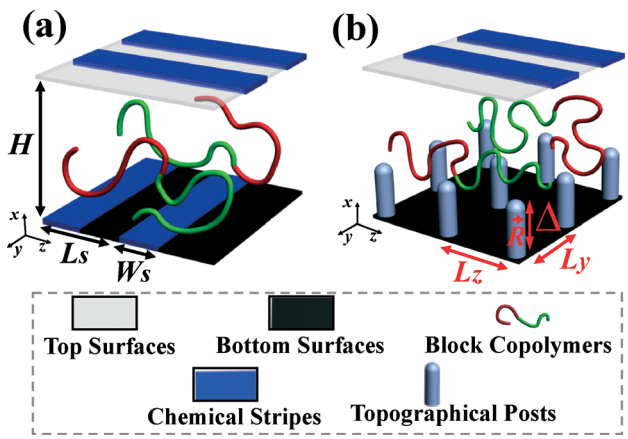

Fig. 1 Simulation setups. (a) Block copolymers confined between two orthogonally oriented chemically patterned surfaces. The patterns comprise periodic stripes with width W_s and periodicity L_s. H represents the film thickness. (b) Block copolymers directed by hybrid templates with chemically and topographically patterned surfaces. An array of posts with height Δ and radius R is located on the bottom surfaces. The periodicities of the post lattice in the y and z directions are specified by L_y and L_z, respectively.

are larger than zero, the interfaces will move towards the top surfaces. Histograms of the position parameters are obtained *via* analyzing a large number of 3D structures in the cell (V_0) collected from different samples. More details about the position parameters are further discussed in Part A of the ESI.†

Fig. 2c displays the probability distributions of the position parameters at different film thicknesses (H = 4.0R_g and H = 6.5R_g). The position parameter histogram at the film thickness of $H \sim 1.0\ L_0$ exhibits a narrow distribution with a single peak at m = 0.0, indicating that the grain interfaces are restricted to the narrow zones at the center of the thin films. When the film thickness (H) is larger than 1.5 L_0, the probability distributions ($P(m)$) are approximately uniform, implying that the grain interfaces fluctuate over a wide range of block copolymer films. We also examine the effects of various parameters, such as the width (W_s) and periodicity (L_s) of the chemical stripes, and the interactions (λN) between the blocks and the chemical stripes on the positions of the grain interfaces (Fig. S2 of the ESI†). It is found that the histograms of the position parameters maintain an approximately uniform distribution in the case of the thick films of the block copolymers.

Fig. 2d depicts the averaged position parameters $\bar{m} \equiv \sum_j P(m_j) m_j$ as a function of film thickness. The averaged position parameters ($\bar{m}$) of the 3D structures approach zero. However, the film thickness has a remarkable effect on the standard deviations (SD(m)) represented by error bars, which are calculated by the equation $\mathrm{SD}(m) \equiv \left(\sum_j P(m_j)(m_j - \bar{m})^2 \right)^{1/2}$. We define the standard deviations SD(m) < 0.1 as 'the narrow zone', which is represented by the filled area in Fig. 2d. In the thin films, there is little room for variation of the position parameters, indicating that the grain interfaces are restricted to the narrow zones of the films. The statistical spreads in the amount of position parameters increase dramatically in the film thickness range $H \geq 5.5R_g$. The main reason is that the difference in the free energies of the 3D structures in the thick films is slight as the position parameters are fluctuated in the range of $-0.30 \leq \bar{m} \leq 0.30$ (Fig. S3 of the ESI†).

In the recent experiments and simulations of de Pablo's group, the morphologies of block copolymers confined between two chemically patterned surfaces were explored.[22,23] The lamellae of symmetric block copolymers are continuously connected by interfaces resembling Scherk's first minimal surfaces. The inset of Fig. 2a displays two representative curves across the saddle points of Scherk surfaces given by the expression $e^{cx}\cos(cy) - \cos(cz) = 0$ with $c = 1.9R_g$. The good agreement between the simulation data and the analytical expression suggests that our SCFT calculations reproduce the surface topologies reported by de Pablo's group. In addition, Monte Carlo simulations of a coarse-grained model corroborate the random distribution behaviors of the grain interfaces, which are consistent with the findings of the SCFT simulations (Fig. 2c).

It should be pointed out that the single templates only consisting of topographical posts on their bottom surfaces cannot guide the symmetric block copolymers to self-assemble into the 3D well-ordered superstructures with internal components. Fig. S4 of the ESI† shows the self-assembled nanostructures of the block copolymers directed by the topographical posts. When the post spacing is commensurate with the natural periodicity of the block copolymer nanostructures, the symmetric block copolymers form the well-ordered lamellae perpendicular to the surfaces. Meanwhile, the in-plane orientations of the vertical lamellae are programmed by the designed parameters of the post arrays.

Next, inspired by the recent works of Ross *et al.*,[11,13] we seek to theoretically engineer hybrid templates containing an array of topographical posts on their bottom surfaces and chemical stripes on their top surfaces (Fig. 1b), which provide a strong thermodynamic driving force for modulating the placements of the grain interfaces in the 3D structures. To elucidate the unique directed self-assembly behaviors and expand on the strategy to achieve controllable morphologies of 3D ordered superstructures over a wide area, large-cell simulations of SCFT for the novel templates are performed.[25] Fig. 3 shows the directed self-assembly behaviors of the block copolymers confined between the top chemically and bottom topographically patterned surfaces. It should be noted that the bottom surfaces are neutral. The periodicities (L_y and L_z) of the post lattice in the y and z directions are fixed at L_y = 3.6R_g and L_z = 3.0R_g, respectively. Since the post spacing L_y satisfies the commensurability conditions of the block

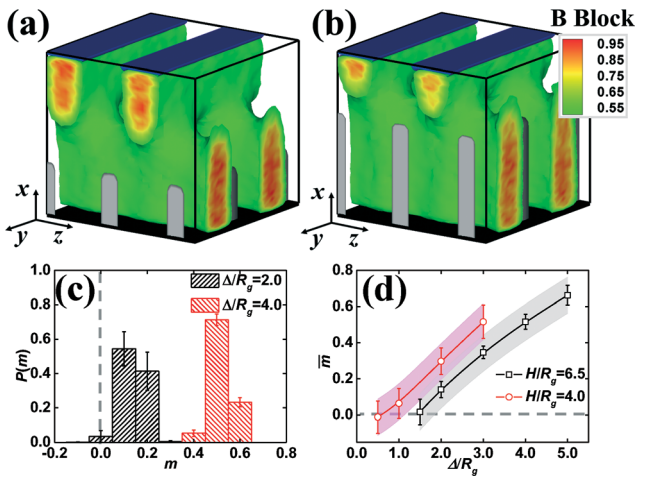

Fig. 3 (a and b) Three-dimensional ordered structures of block copolymers directed by hybrid templates at various post heights ((a) Δ = 2.0R_g and (b) Δ = 4.0R_g). The other model parameters are L_y = 3.6R_g, L_z = 3.0R_g and H = 6.5R_g. In the color bar, the red and green colors represent the B-rich domains and internal interfaces, respectively. The posts are specified by the gray color. Note that only 1/30 part of the simulation box is shown. (c) Probability distributions ($P(m)$) of the position parameter (m) at various post heights (Δ). (d) Averaged position parameters ($\bar{m}$) of the three-dimensional ordered structures as a function of post height (Δ) at various film thicknesses (H). The representations of colors, error bars, dashed lines and filled areas are the same as those of Fig. 2.

copolymer domains, the vertical lamellae in the bottom part of the films are oriented along the z-axis to minimize the strain energy. In the top part of the films, the vertical orientation of the lamellae is preserved and the in-plane orientation of the lamellae is consistent with the y direction of the B-wetting stripes with a width of $W_s = 1.8R_g$ and periodicity of $L_s = 3.6R_g$. As a result, the lamellae with different in-plane orientations meet inside the films and the 3D structures along with the interconnections are also realized in the hybrid topographical-chemical templates (Fig. 3a and b).

Remarkably, the complex 3D architectures in the hybrid templates reveal a new structural feature. As the topographical posts become tall, the grain interfaces are shifted towards the top surfaces of the templates and the corresponding morphologies of the 3D ordered structures are reshaped, as depicted in Fig. 3a and b. To reinforce the impressions from examining the morphologies, the histograms of the position parameters at various post heights are presented in Fig. 3c. Compared with the uniform distributions of the position parameters in the cases of the chemical templates, the distributions of the position parameters of the 3D structures registered by the hybrid templates show a single peak at $m \geq 0$. The observations manifest the fact that the grain interfaces are restricted to the narrow zones in the top part of the thick films. Furthermore, the peak locations of the distributions are tuned by the post height.

To further evaluate the effects of post height on the positions of the grain interfaces, the averaged position parameters are calculated (Fig. 3d). Since the guiding behaviors of the short posts are very similar with the cases of the chemical stripes, the volume fractions of the lamellae with various orientations are roughly equal and therefore the averaged position parameters of the 3D structures registered by the hybrid templates are close to zero. As the height of the topographical posts increases, the bottom part of the block copolymer films remains, but the polymer chains in the top part reassemble in response to the tall posts. Since the dimension L_z of the post lattice is not commensurate with the periodicity of the block copolymer domains, the increased strain energy of the system triggers the rearrangement of the block copolymer domains in the top part of the films, which leads to a decrease in the volume fraction of the lamellae registered by the chemical stripes. Correspondingly, the grain interfaces show a shift towards the top surfaces. As a result, an increase in the post height raises the averaged position parameters of the 3D ordered structures. The same behaviors of the averaged position parameters as a function of post height are inspected in the cases of the thin films with a thickness of $H = 4.0R_g$. Another important outcome shown in Fig. 3d is that the standard deviations from the averaged position parameters are less than 0.1, suggesting that the grain interfaces can be localized in the narrow zones of the films. Given these observations, robust control over the morphologies of the 3D sophisticated structures and the placements of the grain interfaces is properly achieved by integrating the chemically and topographically patterned surfaces.

It is also important to comprehend the roles of other parameters of the templates, such as the periodicities (L_y and L_z) of the topographical posts and the dimension (W_s and L_s) of the chemical stripes, on the directed self-assembly behaviors of the block copolymer films. To clarify these issues, the averaged position parameters of the 3D ordered structures as functions of L_y and L_s are shown in Fig. 4a and b, respectively. When the periodicity L_y of the post lattice does not satisfy the commensurability conditions, the domains of the block copolymers directed by the posts possess a higher free energy due to a tensile or compressive strain to fit within the post array. To relieve the deformation of the lamellae, the grain interfaces move towards the bottom surfaces. This leads to a decrease in the averaged position parameters as the commensurability conditions are not satisfied (Fig. 4a). Similarly, as the periodicity L_s of the chemical stripes deviates from the commensurability conditions, the grain interfaces move towards the top chemically patterned surfaces to alleviate the energy contributions from the compressed or elongated lamellae (Fig. 4b). It should be mentioned that the interface positions are also tuned by the stripe width. These results suggest that the commensurability conditions could be exploited to manipulate the placements of the grain interfaces and the corresponding morphologies of the 3D superstructures. The findings provide significant guidance for experimentalists to select the geometry parameters of hybrid templates to engineer 3D ordered structures with tunable internal components.

It should be noted that the chemical selectivity of the bottom surfaces has effects on the morphologies and orientations of the self-assembled structures programmed by the topographical templates and the hybrid templates (Fig. S5 and S6 of the ESI†). When the bottom surfaces strongly repel the B blocks, A-rich flat layers are produced in the bottom part of the films and destabilize the 3D well-ordered structures of the vertical lamellae.

On the basis of the tunable in-plane orientations of the lamellae registered by the rectangular lattice of the topographical

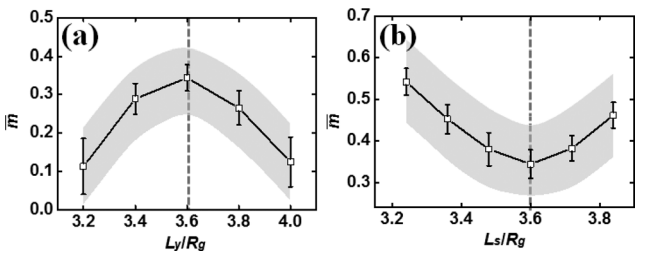

Fig. 4 (a) Averaged position parameters ($\bar{m}$) of the three-dimensional ordered structures as a function of periodicity (L_y) of the post lattice in the y direction. Note that the dimension of the chemical stripes satisfies the commensurability conditions. (b) Averaged position parameters ($\bar{m}$) of three-dimensional ordered structures as a function of periodicity (L_s) of the stripes. The periodicities of the post lattice are $L_y = 3.6R_g$ and $L_z = 3.0R_g$. The dashed lines indicate the cases where the periodicities of the post lattices or stripes satisfy the commensurability conditions of the block copolymer domains. The filled areas represent the standard deviations SD(m) < 0.1.

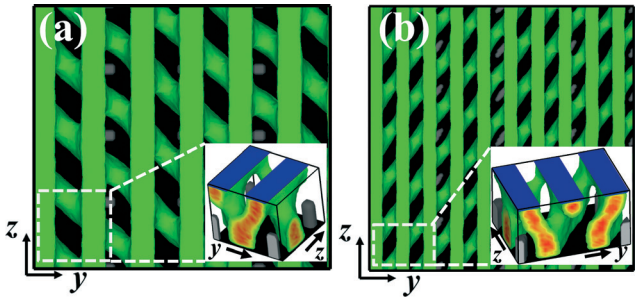

Fig. 5 Top-down views of the three-dimensional structures of lamellae with tunable orientations through changing periodicities L_y and L_z of the post lattice. (a) $L_y = 5.4R_g$ and $L_z = 4.8R_g$ and (b) $L_y = 9.0R_g$ and $L_z = 6.0R_g$. Note that the topographical posts in image (b) have an elliptical shape. Insets are the three-dimensional views of the local structures enclosed in the dashed boxes. Only 1/16 and 1/24 portions of the simulation cells are shown in insets (a) and (b), respectively.

posts (Fig. S4 of the ESI†), the hybrid topographical-chemical templates provide a new route to construct non-orthogonally crossed lamellar structures without additional treatments required on the chemically patterned surfaces. In order to demonstrate this ability, simulations for the hybrid templates with a series of periodicities of the post lattice are carried out. As predicted from the commensurability conditions, the vertical lamellae near the bottom surfaces align diagonally with respect to the post lattice when the post spacings are set as $L_y = 5.4R_g$ and $L_z = 4.8R_g$. Combining the lamellae registered by the chemically patterned surfaces, one obtains non-orthogonally crossed structures (Fig. 5a). When the spacing of the posts further increases, the block copolymers self-assemble into poorly ordered patterns. As shown in Fig. S7 of the ESI,† lamellae with degenerate orientations appear due to the isotropic characteristics of the circular posts. To achieve highly ordered superstructures, one promising strategy is the introduction of anisotropic posts with an elliptical shape,[25] which provide additional in-plane orientation guidance. As demonstrated in Fig. 5b, the bock copolymers guided by the hybrid templates with elliptical posts self-assemble into crossed superstructures with a single in-plane orientation in the bottom part of the films.

Finally, we would like to emphasize that the local structures of the grain interfaces are highly degenerate and have different possible morphologies or geometries due to the frustrated features of the 3D superstructures with distinct lamellar orientations.[22,27,28] For example, Gido *et al.* experimentally found that both the morphologies of Scherk's surfaces and helicoid sections exist in intersecting lamellar nanodomains at low twist angles, and theoretically demonstrated that the energies of both morphologies are comparable in this twist range.[29–31] These findings provide a valuable clue for exploring the interfacial structures of lamellar grains (*i.e.*, besides Scherk's surfaces, helicoid section morphologies of the grain interfaces possibly emerge in the non-orthogonally crossed structures, as shown in Fig. 5). It should be mentioned that in comparison with the approach proposed by Gido and co-workers, the SCFT used here provides a powerful tool for screening the novel local morphologies of complex superstructures such as helicoid sections,[31] connected tubes,[22] and Schwarz P phases.[32] Future studies based on SCFT will be devoted to elucidating in more detail the structural characteristics of grain interfaces in frustrated superstructures including the vertical interconnections between the top and bottom lamellae as well as the mean and Gaussian curvatures of local structures.

Conclusions

In summary, we theoretically propose and demonstrate a new category of templates to guide the self-assembly of block copolymers. Our large-cell simulations of SCFT predict that by collaborating with the top chemically patterned surfaces, the topographical posts in the bottom surfaces direct the symmetric block copolymers to self-assemble into the 3D long-range ordered superstructures with controllable morphologies and predictable placements of grain interfaces. The positions of the grain interfaces are strongly dependent on the post height and flexibly adjusted by the commensurability conditions. Additionally, the 3D structures of lamellae with non-orthogonal orientations are successfully constructed by simply modulating the periodicities of the post arrays. The above findings indicate that incorporating the topographical posts into the template design significantly enhances the regulation of the 3D well-ordered structures, which gains access to novel materials with tunable properties *via* the rational self-assembly of smart block copolymers.

Acknowledgements

This work was supported by the National Natural Science Foundation of China (51203049, 21574040 and 21234002), and the Fundamental Research Funds for the Central Universities. Support from 111 project (B14018) is also appreciated.

Notes and references

1 C. A. Ross, K. K. Berggren, J. Y. Cheng, Y. S. Jung and J.-B. Chang, *Adv. Mater.*, 2014, **26**, 4386.
2 M. S. Onses, C. Song, L. Williamson, E. Sutanto, P. M. Ferreira, A. G. Alleyne, P. F. Nealey, H. Ahn and J. A. Rogers, *Nat. Nanotechnol.*, 2013, **8**, 667.
3 G. von Freymann, A. Ledermann, M. Thiel, I. Staude, S. Essig, K. Busch and M. Wegener, *Adv. Funct. Mater.*, 2010, **20**, 1038.
4 W. Lu and C. M. Lieber, *Nat. Mater.*, 2007, **6**, 841.
5 M. Luo and T. H. III Epps, *Macromolecules*, 2013, **46**, 7567.
6 C. M. Bates, M. J. Maher, D. W. Janes, C. J. Ellison and C. G. Willson, *Macromolecules*, 2014, **47**, 2.
7 S. X. Ji, U. Nagpal, W. Liao, C.-C. Liu, J. J. de Pablo and P. F. Nealey, *Adv. Mater.*, 2011, **23**, 3692.
8 P. Chen, H. Liang, R. Xia, J. Qian and X. Feng, *Macromolecules*, 2013, **46**, 922.
9 S.-J. Jeong, H.-S. Moon, J. Shin, B. H. Kim, D. O. Shin, J. Y. Kim, Y. H. Lee, J. U. Kim and S. O. Kim, *Nano Lett.*, 2010, **10**, 3500.

10 S. Y. W. Kim, A. Nunns, G. Gwyther, R. L. Davis, I. Manners, P. M. Chaikin and R. A. Register, *Nano Lett.*, 2014, **14**, 5698.
11 J. K. Yang, Y. S. Jung, J. B. Chang, R. A. Mickiewicz, A. Alexander-Katz, C. A. Ross and K. K. Berggren, *Nat. Nanotechnol.*, 2010, **5**, 256.
12 I. Bita, J. K. W. Yang, Y. S. Jung, C. A. Ross, E. L. Thomas and K. K. Berggren, *Science*, 2008, **321**, 939.
13 K. G. A. Tavakkoli, K. W. Gotrik, A. F. Hannon, A. Alexander-Katz, C. A. Ross and K. K. Berggren, *Science*, 2012, **336**, 1294.
14 K. W. Gotrik, T. Lam, A. F. Hannon, W. Bai, Y. Ding, J. Winterstein, A. Alexander-Katz, J. A. Liddle and C. A. Ross, *Adv. Funct. Mater.*, 2014, **24**, 7689.
15 V. F. Pavlidis and E. G. Friedman, *Proc. IEEE*, 2009, **97**, 123.
16 X. Cao, L. Zhang, J. Gu, L. Wang and J. Lin, *Polymer*, 2015, **72**, 10.
17 M. P. Stoykovich, M. Müller, S. O. Kim, H. H. Solak, E. W. Edwards, J. J. de Pablo and P. F. Nealey, *Science*, 2005, **308**, 1442.
18 R. Ruiz, H. Kang, F. A. Detcheverry, E. Dobisz, D. S. Kercher, T. R. Albrecht, J. J. de Pablo and P. F. Nealey, *Science*, 2008, **321**, 936.
19 X. Ye, B. J. Edwards and B. Khomami, *Macromolecules*, 2010, **43**, 9594.
20 F. A. Detcheverry, G. Liu, P. F. Nealey and J. J. de Pablo, *Macromolecules*, 2010, **43**, 3446.
21 Q. Wang, *Macromol. Theory Simul.*, 2005, **14**, 96.
22 A. Ramírez-Hernández, G. Liu, P. F. Nealey and J. J. de Pablo, *Macromolecules*, 2012, **45**, 2588.
23 G. Liu, A. Ramírez-Hernández, H. Yoshida, K. Nygård, D. K. Satapathy, O. Bunk, J. J. de Pablo and P. F. Nealey, *Phys. Rev. Lett.*, 2012, **108**, 065502.
24 G. H. Fredrickson, *The Equilibrium Theory of Inhomogeneous Polymers*, Oxford University Press, Oxford, 2006.
25 L. Zhang, L. Wang and J. Lin, *ACS Macro Lett.*, 2014, **3**, 712.
26 M. Müller, *Phys. Rev. Lett.*, 2012, **109**, 087801.
27 E. L. Thomas, D. M. Anderson, C. S. Henkee and D. Hoffman, *Nature*, 1988, **334**, 598.
28 H. Jinnai, K. Sawa and T. Nishi, *Macromolecules*, 2006, **39**, 5815.
29 S. P. Gido, J. Gunther, E. L. Thomas and D. Hoffman, *Macromolecules*, 1993, **26**, 4506.
30 S. P. Gido and E. L. Thomas, *Macromolecules*, 1994, **27**, 849.
31 S. P. Gido and E. L. Thomas, *Macromolecules*, 1997, **30**, 3739.
32 M. Beluskin and G. Gompper, *J. Chem. Phys.*, 2009, **130**, 134712.

